

Supplementary Information for

Earth Abundant Perovskite Oxides for Low Temperature CO₂ Conversion

Debtanu Maiti, Bryan J. Hare, Yolanda A. Daza, Adela E. Ramos, John N. Kuhn*,
Venkat R. Bhethanabotla*

Department of Chemical & Biomolecular Engineering, University of South Florida,
Tampa, FL 33620.

*Correspondence to: bhethana@usf.edu; jnkuhn@usf.edu

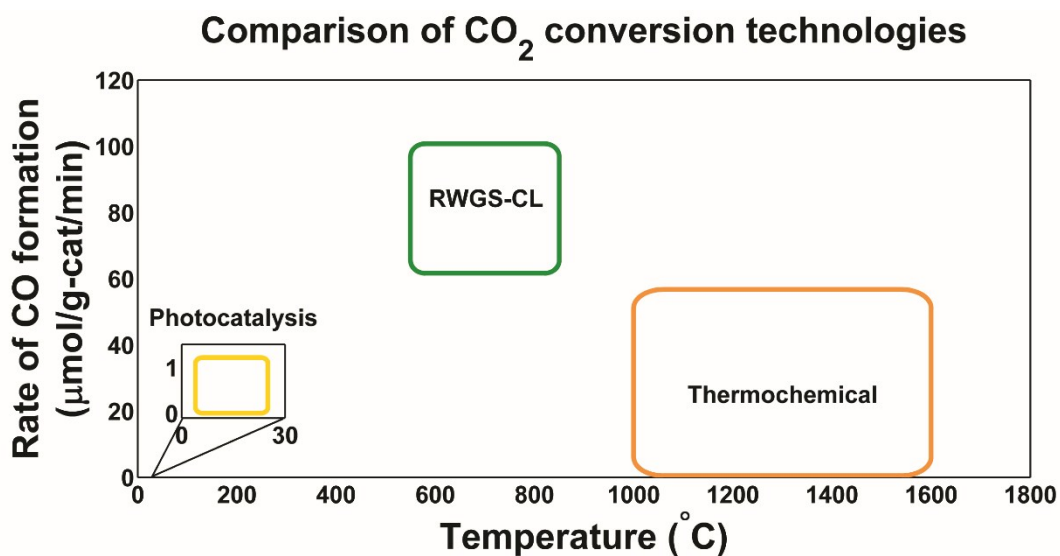


Fig. S1. Comparison of CO₂ conversion rates and operation temperatures of photocatalytic, thermochemical and RWGS-CL processes.

The data for the temperature of operation and the product formation rates has been based on the literature values (13 – 26, 30, 31, 45 – 49). Detailed information is documented in Table S1.

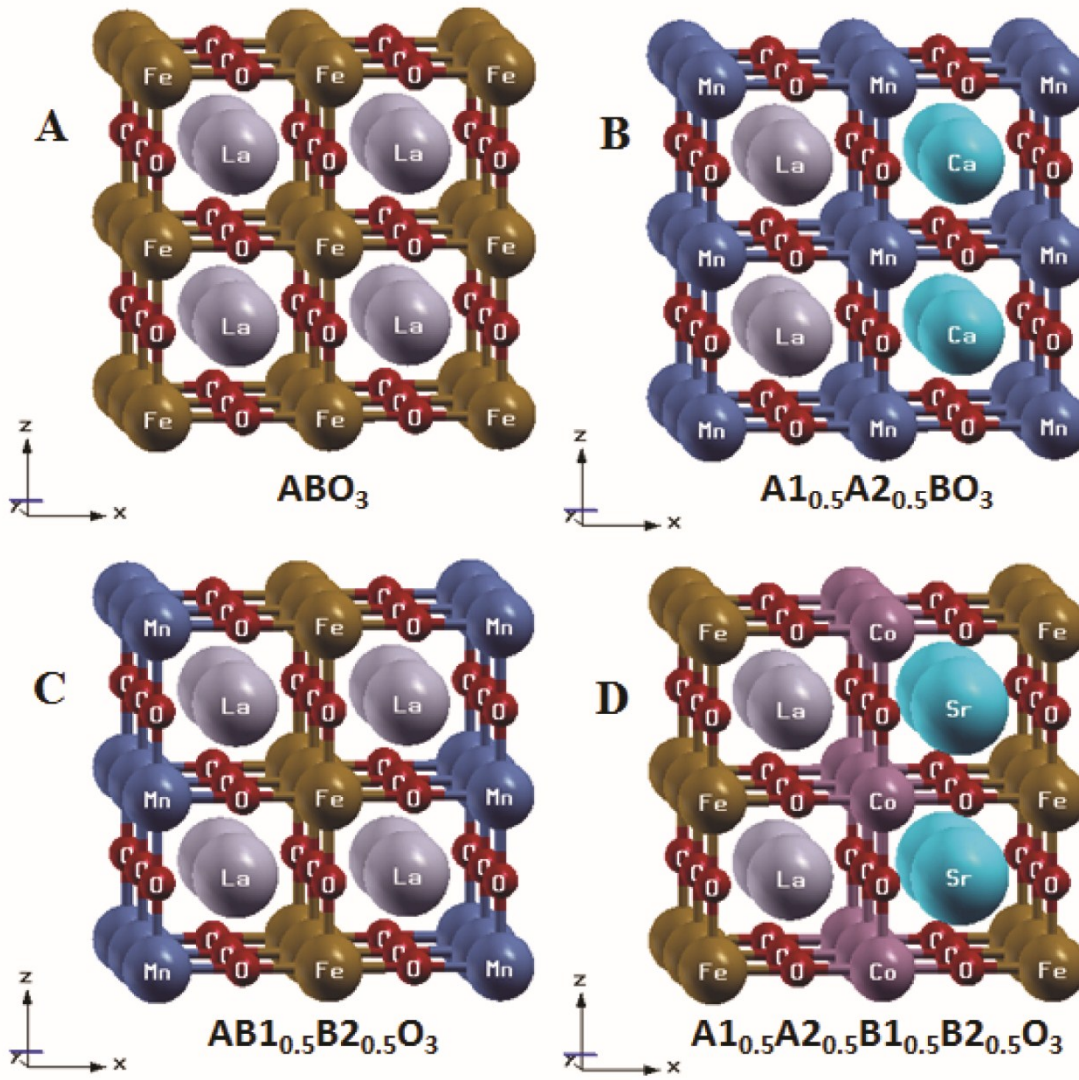


Fig. S2. Representative relaxed crystal structures of (A) ABO_3 , (B) $A_{1.5}A_{2.5}BO_3$, (C) $AB_{1.5}B_{2.5}O_3$, and (D) $A_{1.5}A_{2.5}B_{1.5}B_{2.5}O_3$.

The crystal structures (as in Fig. S2) are the cubic crystals of the perovskite oxides. The atomic configurations within the crystal lattice has been optimized based on the minimum energy structure for some selective ABO_3 , $A_{1.5}A_{2.5}BO_3$, $AB_{1.5}B_{2.5}O_3$, and $A_{1.5}A_{2.5}B_{1.5}B_{2.5}O_3$ structures.

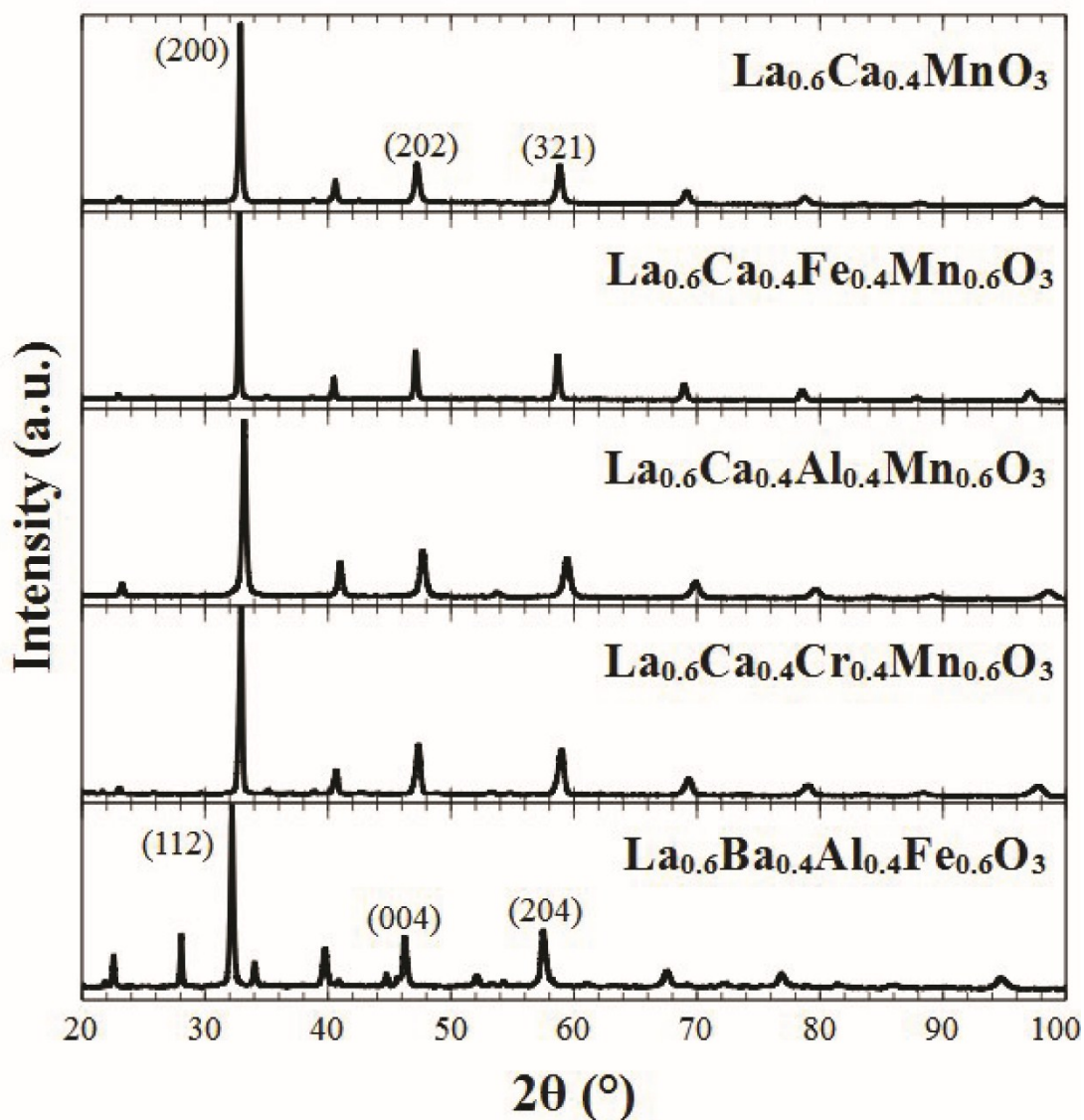


Fig. S3. XRDs of samples that exhibited higher CO yields than $\text{La}_{0.75}\text{Sr}_{0.25}\text{FeO}_3$, each of which demonstrated a dominant perovskite crystalline structure with orthorhombic geometry (Reference code: 00-046-0513, space group: Pnma). Slight rightward shifts of major $\text{La}_{0.6}\text{Ca}_{0.4}\text{MnO}_3$ diffraction lines suggest successful incorporation of additional ‘B’ site elements without notable formation of secondary oxide phases

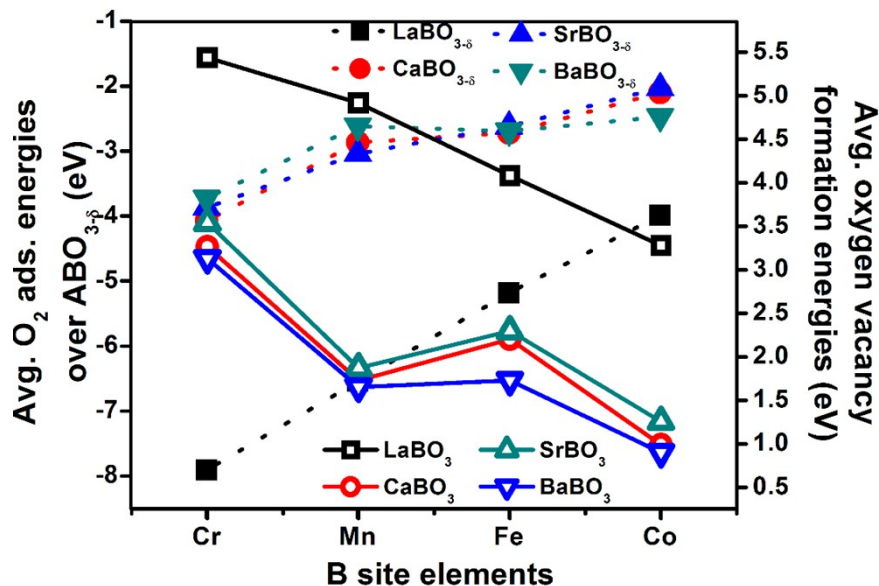


Fig. S4. Comparison of oxygen vacancy formation energy (E_{vac}) and O_2 adsorption energy (E_{ads}) over perovskite oxides (ABO_3): dotted line represents the E_{ads} while solid lines represent E_{vac} . The decreasing trend of both the material properties led us to propose E_{vac} as the sole descriptor for RWGS-CL. Too high E_{vac} represents the reluctance of materials to lose oxygen thereby requiring high temperatures for the reduction process. While too low E_{vac} values mark easy formation of vacancies (can be generated at low temperatures) with materials being too stable in oxygen-deficient forms to convert CO_2 to CO . Thus, this calls for an optimum E_{vac} (which translates to optimum E_{ads}) which can allow CO_2 conversion at sustainable temperatures.

Oxygen vacancy formation energies of $\text{La}_{0.5}\text{Ca}_{0.5}\text{Mn}_{0.75}\text{Fe}_{0.25}\text{O}_3$

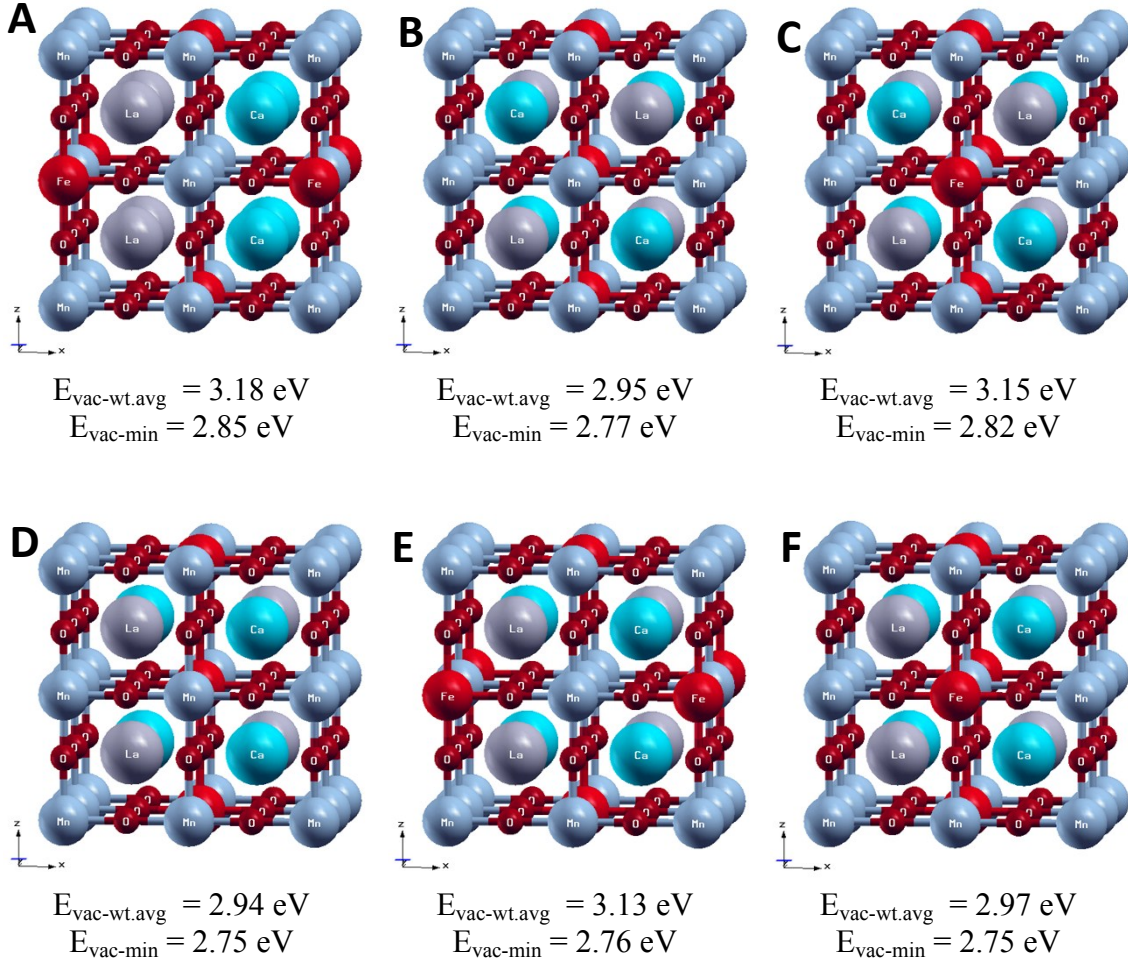


Fig. S5. Lattice configuration dependent oxygen vacancy formation energy (E_{vac}) variation for $\text{La}_{0.5}\text{Ca}_{0.5}\text{Mn}_{0.75}\text{Fe}_{0.25}\text{O}_3$ perovskite oxide. Site weighted oxygen vacancy formation energy ($E_{\text{vac-wt.avg}}$) and oxygen vacancy formation energy at the least resistant site ($E_{\text{vac-min}}$) for different atomic orderings (A-F) in the crystal lattice of $\text{La}_{0.5}\text{Ca}_{0.5}\text{Mn}_{0.75}\text{Fe}_{0.25}\text{O}_3$.

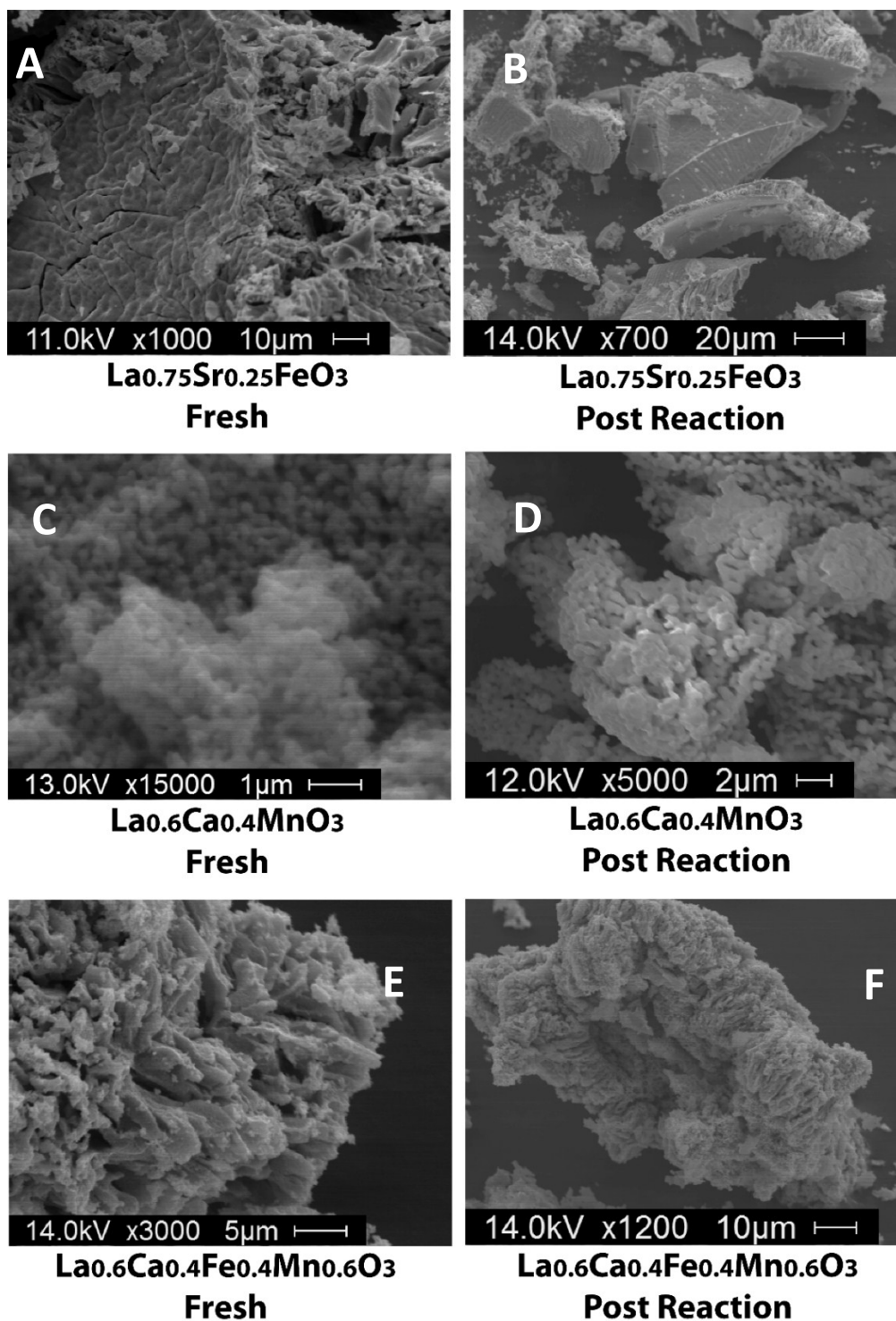


Fig. S6. SEM images of different perovskite oxides at two different conditions: Freshly prepared (A, C, E) and at post reaction condition (B, D, F). Three different samples showing good CO₂ conversion performance were probed – La_{0.75}Sr_{0.25}FeO₃ (A, B), La_{0.6}Ca_{0.4}MnO₃ (C, D), and La_{0.6}Ca_{0.4}Fe_{0.4}Mn_{0.6}O₃ (E, F),

Table S1. Comparison of CO₂ conversion performance by various catalysts by various methods at different operational temperatures.

Author Information (Reference)	Material	Method	Temp (°C)	Rates (μmoles/g cat/min)
Izumi et al. (13)	TiO ₂ (P25)	Photocatalysis	5	0.006
Izumi et al. (13)	Pt-Ti_Y_Zeolite	Photocatalysis	55	0.00133
Izumi et al. (13)	Ru/RuO _x /TiO ₂	Photocatalysis	46	0.817
Izumi et al. (13)	Cu-ZnO	Photocatalysis	32-40	0.0005
Huang et al. (19)	Co ₃ O ₄ /CeO ₂	Photocatalysis	RT	0.1045
Chueh et al. (10)	Ceria	Thermochemical	1500/900	206 (peak) 81 (avg)
Mc Daniel et al. (24)	Sr _{0.6} La _{0.4} Mn _{0.6} Al _{0.4} O ₃	Thermochemical	1350/1000	9.3
Mc Daniel et al. (24)	Sr _{0.4} La _{0.6} Mn _{0.4} Al _{0.6} O ₃	Thermochemical	1350/1000	18.4
Mc Daniel et al. (24)	Sr _{0.4} La _{0.6} Mn _{0.6} Al _{0.4} O ₃	Thermochemical	1350/1000	21.9
Miller et al. (21)	Ce _{0.67} Fe _{2.33} O ₄	Thermochemical	1400/1100	0.5
Lorentzou et al. (18)	Ni-Ferrite	Thermochemical	1100	22
Inoue et al. (17)	Rh/TiO ₂	RWGS	300	56.0
Ginés et al. (22)	Commercial Cu/ZnO/Al ₂ O ₃	RWGS	250	258.6
Galvita et al. (16)	Ce _{0.2} Fe _{0.8} O ₂	RWGS-CL	750/600	210
Rihko- Struckmann et al. (48)	Fe ₂ O ₃ :Al ₂ O ₃ (Fe:Al=7:3)	RWGS-CL	750	440
Rihko- Struckmann et al. (48)	Fe ₂ O ₃ :Al ₂ O ₃ (Fe:Al=9:1)	RWGS-CL	750	350
Wenzel et al. (49)	Fe ₃ O ₄ - Ce _{0.5} Zr _{0.5} O ₂	RWGS-CL	800	22.22
Daza et al. (14)	La _{0.75} Sr _{0.25} CoO ₃	RWGS-CL	500/850	100.8
Daza et al. (15)	La _{0.75} Sr _{0.25} FeO ₃	RWGS-CL	550	80

Table S2. CO₂ conversion rates and yield in the RWGS-CL process using perovskite oxides.

Material	CO yield (μmoles/g cat)	Maximum CO production rate (μmoles/g cat/min) [corresponding temperature(°C)]	CO production onset temperature (° C)	% CO ₂ conversion *
La _{0.75} Sr _{0.25} FeO ₃	599	60.5 [560]	450	2.02
La _{0.6} Ca _{0.4} MnO ₃	1242	113 [710]	585	1.82
La _{0.6} Ca _{0.4} Fe _{0.4} Mn _{0.6} O ₃	973	160 [500]	450	2.40
La _{0.6} Ca _{0.4} Al _{0.4} Mn _{0.6} O ₃	757	38.0 [640]	550	0.88
La _{0.6} Ba _{0.4} Fe _{0.6} Al _{0.4} O ₃	569	77.4 [550]	440	1.22
La _{0.6} Ca _{0.4} Cr _{0.4} Mn _{0.6} O ₃	566	18.3 [680]	450	0.42
La _{0.6} Ca _{0.4} Cr _{0.6} Al _{0.4} O ₃	288	10.0 [750]	535	0.23
La _{0.6} Ca _{0.4} Cr _{0.6} Fe _{0.4} O ₃	257	6.70 [860]	500	0.14
La _{0.6} Ba _{0.4} Mn _{0.6} Fe _{0.4} O ₃	254	11.4 [860]	650	0.15
La _{0.6} Ba _{0.4} MnO ₃	210	16.1 [640]	580	0.33
La _{0.6} Ba _{0.4} Mn _{0.6} Cr _{0.4} O ₃	198	18.5 [610]	535	0.37
La _{0.6} Ba _{0.4} Cr _{0.8} Co _{0.2} O ₃	196	8.60 [630]	525	0.31
La _{0.6} Ca _{0.4} Cr _{0.8} Co _{0.2} O ₃	146	9.80 [690]	560	0.22
La _{0.6} Ba _{0.4} Cr _{0.6} Fe _{0.4} O ₃	135	8.50 [560]	470	0.18

The notable aspect of these perovskite oxides is that, even if the peak CO formation rates for some of the oxides may happen at a higher temperature, the onset temperature is mostly between 450 °C – 550 °C. This provides ample opportunity for further tuning of the composition of these materials to enhance CO conversion at lower temperatures.

*These CO₂ conversion data must not be confused as a process limitation. We hereby state that shorter reaction timescales (in the form of pulses) along with optimizing the CO₂ feed volumetric rate can enhance these conversion values by several orders.